Title

SPECTROSCOPY OF 140Ce and 138Ce VIA THE 14OCe(p,p'), 142Ce(p,t), and !40Ce(p,t) REACTIONS AT E = 30 MeV

Author

Sherman, J.D.

Publication Date

1976-10-01

Submitted to Physical Review C

LBL-4379
Preprint

SPECTROSCOPY OF ^{140}Ce AND ^{138}Ce VIA THE ^{140}Ce(p, p'), ^{142}Ce(p, t), AND ^{140}Ce(p, t) REACTIONS AT E_p = 30 MeV

J. D. Sherman, D. L. Hendrie
and M. S. Zisman

October 1976

Prepared for the U. S. Energy Research and
Development Administration under Contract W-7405-ENG-48

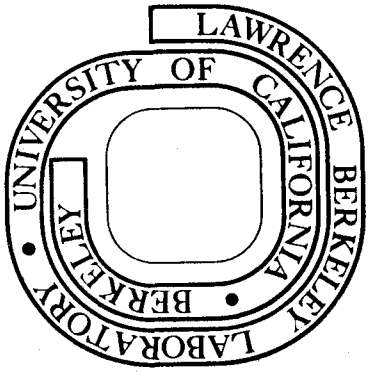

DISCLAIMER

SPECTROSCOPY OF ^{140}Ce AND ^{138}Ce VIA THE ^{140}Ce(p,p'), ^{142}Ce(p,t), AND ^{140}Ce(p,t) REACTIONS AT E_p = 30 MeV*

J. D. Sherman†, D. L. Hendrie,
and M. S. Zisman

Lawrence Berkeley Laboratory
University of California
Berkeley, California 94720

October 1976

ABSTRACT

The nuclei ^{138,140}Ce have been studied by means of the ^{140}Ce(p,t), ^{142}Ce(p,t) and ^{140}Ce(p,p') reactions at 30 MeV. Angular distributions have been measured from θ_{lab} = 16° to 64°. The inelastic scattering data were analyzed with DWBA to confirm multipolarities and extract deformation parameters for the strongly excited levels. The (p,t) data were also analyzed with DWBA to obtain limits on the two-nucleon orbital angular momentum (L) transfer. This analysis, plus the empirical angular distribution shapes of levels with known J^π, permit us to suggest (or at least limit) J^π values for many new levels. The (p,t) differential cross sections have been further analyzed in terms of simple two neutron configurations through the enhancement factor concept. The two neutron transfer results are discussed in terms of the pair vibration model.

[NUCLEAR REACTIONS: ^{142,140}Ce(p,t), ^{140}Ce(p,p'), E_p = 30 MeV; measured level energies and $\sigma(\theta)$; DWBA analysis, deformation parameters, enhancement factors.]

I. INTRODUCTION

Previous investigations[1-3] of the (p,t) reaction on the Ce isotopes have been directed mainly toward investigating the usefulness of a pairing vibrational model interpretation[4] at the N = 82 closed shell. Consequently, a detailed analysis of the spectroscopic information available from the (p,t) reaction on ^{142}Ce and ^{140}Ce targets has not been given up to now. The combination of high beam energy, good energy resolution, and reasonably characteristic angular distributions which hold for the present (p,t) experiments makes such an analysis possible. The ^{140}Ce(p,p') experiment, done simultaneously with the ^{140}Ce(p,t) reaction, is also reported here. This reaction is of interest to compare with the isoscalar[5] excitation of collective levels in ^{140}Ce as well as comparing with other inelastic proton scattering measurements on N=82 nuclei.[6,7] A report on part of the data discussed here is given in Ref. 2.

II. EXPERIMENT

A. Targets

Self-supporting 1.9 cm diameter targets of ^{142}Ce (0.40 mg/cm^2, 90% enriched) and ^{140}Ce (0.79 mg/cm^2, 99.5% enriched) were used in these experiments. All handling of the Ce targets was done in an Ar atmosphere and the targets were kept in vacuum for long term storage. Details of the target preparation may be found in Ref. 8.

B. Experimental Procedure

The experiments were carried out with a 30.3 MeV proton beam obtained from the Lawrence Berkeley Laboratory 88-Inch Cyclotron high resolution beam line.[9] The data were measured in a 91 cm diameter scattering chamber by means of a pair of two-counter telescopes. For the ^{142}Ce + p experiment, 250 μm ΔE

Si(P) and 3 mm E Si(Li) detectors were used, while for ^{140}Ce + p experiments, 5 mm Si(Li) counters were used. Cooling of the detectors to -25°C was accomplished by means of thermoelectric coolers. The ΔE-E signals fed a Goulding-Landis[10] particle identifier which produced good separation of the charge one reaction products. A split Faraday cup, mounted approximately 1.5 meters from the target position, monitored the directional stability of the beam as well as providing charge integration. Target thickness monitoring was accomplished by a fixed-angle detector mounted in the scattering chamber.

Figures 1 and 2 show triton spectra from the ^{142}Ce(p,t) and ^{140}Ce(p,t) reactions, respectively. The energy resolution in the ^{142}Ce experiment was 30 keV (FWHM) while in the ^{140}Ce experiment it was about 55 keV. Triton and proton angular distributions (Figs. 3-6) were measured between 16° and 64° (lab).

C. Data Calibration

1. ^{140}Ce(p,p')

The ^{140}Ce(p,p') spectra were calibrated on the basis of known ^{140}Ce excitation energies[11,12] as well as several proton groups arising from light target impurities. The results are given in Table I, where they are compared with the ^{140}Ce(α,α') experiment.[5] The proton energy resolution limited analysis to the strongly excited states in ^{140}Ce.

2. ^{142}Ce(p,t)

These spectra were calibrated using γ-decay results[11,12] as well as two impurity peaks from the ^{19}F(p,t)^{17}F reaction. (see Fig. 1). The calibration covered the full range of excitations observed in the ^{142}Ce(p,t)^{140}Ce reaction, and extrapolations were not necessary. The ^{142}Ce(p,t) spectra yielded a total of 45 levels in ^{140}Ce. These are listed in Table II, where they are compared with previous results for the ^{140}Ce level structure.

3. ^{140}Ce(p,t)

The energy calibration of the ^{138}Ce data relied on accurate excitation energies derived from γ-decay studies.[13] The average excitation energies of the 21 observed levels are listed in Table III, along with results from earlier work. The 10% ^{140}Ce impurity in the ^{142}Ce target allowed the ^{140}Ce(p,t) Q-value to be measured relative to that for the ^{142}Ce(p,t) reaction. The result we obtained was -8.167±0.020 MeV, in good agreement with previous values.[3,14]

D. Normalization

Absolute cross sections from the ^{140}Ce target were obtained by two methods. The first method involved a direct weighing of the target along with accurate measurement of the detector solid angles. The second method involved normalizing the measured elastic scattering angular distribution to optical model predictions. The optical parameters chosen were obtained from a global analysis[15] of proton elastic scattering and are given as set P1 in Table IV. These two methods agreed to 5%. Since no elastic proton data were taken on the ^{142}Ce target, this normalization was obtained only from the target weight.

Dead time corrections were made with pulser signals triggered by the monitor detector; the monitor was also used to normalize the data from angle to angle. The absolute cross sections displayed in Figs. 3-6 are estimated to have an uncertainty of ± 10%.

III. ANALYSIS AND DISCUSSION

A. ^{140}Ce(p,p')

The proton inelastic scattering results are given in Table I and Fig. 3. Good agreement with excitation energies and J^{π} assignments was found with the ^{140}Ce(α,α') work.[5] We did not observe the 2.35 MeV and 3.04 MeV

levels reported there; it is likely that the better resolution (35 keV) of the (α,α') experiment allowed identification of these weakly excited levels.

In previous studies[6,7] of inelastic scattering of 30 MeV protons from ^{138}Ba and ^{144}Sm (also N = 82), it was found that the angular distribution shapes are characteristic of the orbital angular momentum transfer (L). Since these are $J^{\pi} = 0^{+}$ targets, spin-parity values could then be obtained through use of the natural-parity selection rules, $J_f = L$ and $\pi_f = (-)^L$, where J_f and π_f are the spin and parity of the excited state. These empirical angular distribution shapes are shown as dashed lines in Fig. 3 for levels with $J^{\pi} = 2^{+}$, 3^{-}, and 4^{+}. Good agreement between the shapes determined in Refs. 6 and 7 and our ^{140}Ce(p,p') data is found for the L = 2 and L = 3 transitions, while the L = 4 shape is qualitatively similar.

The ^{140}Ce(p,p') angular distributions were analyzed using a collective model form factor[16] in a DWBA calculation. In this theory, the optical model analysis of the proton elastic scattering determines all parameters except the deformation parameter β_L which normalizes the distorted wave predictions ($\sigma_{DW}(\Theta)$) to the experimental differential cross sections ($\sigma_{exp}(\Theta)$) by the relation

$$\sigma_{exp}(\Theta) = \beta_L^2 \, \sigma_{DW}(\Theta) \ . \qquad (1)$$

The $\sigma_{DW}(\Theta)$ were calculated using the code DWUCK74.[17] Detailed formulae for evaluation of $\sigma_{DW}(\Theta)$ have been given in the literature.[5,16-18]

The solid curves shown in Fig. 3 are DWBA predictions using proton optical model parameters taken from the literature[15] (and listed as set P1 in Table IV). The form factor included a Coulomb excitation contribution[16] as well as real and imaginary nuclear terms. This last term has improved theoretical comparisons with experiments involving inelastic scattering of protons,[19] ^{3}He,[20] and ^{4}He[21] particles. Inclusion of the imaginary term also affected the β_L values extracted from the data;[19-21] in particular, the β_3 for the 2.469 MeV

level and the β_2 for the 2.902 MeV state were decreased by about 30% compared to the values obtained from the analysis using only a real form factor. Excluding the Coulomb excitation term caused the first maximum of the L = 2 angular distribution to shift (by 3°) to smaller angles without significantly changing the magnitude, while the L = 3 prediction was hardly influenced.

The DWBA normalizations to experiment are given in Table I in terms of the deformation lengths[22] $\delta_L = \beta_L R_R$, where $R_R = 1.17\ A^{1/3}$. The isoscalar transition rates in single particle units were calculated from

$$G_{IS}\ (L,0 \rightarrow L) = \frac{Z^2}{4\pi}\ \frac{(L+3)^2}{(2L+1)}\ \left(\frac{\beta_L R_R}{R_u}\right)^2 \quad , \qquad (2)$$

where $R_u = 1.2\ A^{1/3}$ is the uniform mass radius.[23] These isoscalar transition rates are compared with the ^{140}Ce(α,α') results in Table I. Good agreement between the two experiments is found for the 2^+ and 4^+ states. The odd parity levels (2.469 MeV 3^- and 3.264 MeV 5^-) are not in such good agreement, although the δ_3 values extracted for the 2.469 MeV level from the two experiments are consistent within errors. The 3^- isoscalar transition strength derived from (p,p') is 40% greater than that from (α,α') and is nearly the same as the electromagnetic transition rate.[24]

B. ^{142,140}Ce(p,t) ^{140,138}Ce

1. DWBA Analysis

Triton angular distributions from (p,t) reactions are known to reflect the total orbital angular momentum (L) of the two picked-up neutrons.[25] The zero-range single step DWBA treatment[26-28] of two-nucleon transfer reactions is generally successful at providing a reasonable description of angular distribution shapes for vibrational nuclei,[29] although for permanently deformed nuclei calculations including inelastic processes are different in shape from DWBA predictions.[30] Further, finite-range DWBA[31,32] does not seem to differ from the zero-range DWBA as regards angular distribution shape. Thus, by using zero-range DWBA angular distribution predictions as a guide to assigning L transfers, along with the natural-parity selection rules for a $J^{\pi} = 0^{+}$ target, J^{π} values or at least J^{π} limits can be assigned to many of the levels observed in the ^{142}Ce(p,t) and ^{140}Ce(p,t) reactions. Wherever possible, empirical angular distributions are also used as a supplemental aid in assigning multipolarities to states with unknown J^{π}.

A comprehensive discussion of parameters that are required for a zero-range DWBA calculation of the (p,t) reaction has been given.[25] In that work the DWBA predictions were not very sensitive to the choice of optical model and form factor parameters, although significant changes in the angular distribution shapes were noted when configuration-mixed wave functions caused destructive interference at the nuclear surface. Since our conclusions concerning parameter sensitivity were not appreciably different from those of Ref. 25, we will not discuss this point in detail here.

Straightforward assumptions about the required parameters resulted in favorable comparisons between the calculations and experimental results for levels in ^{140}Ce and ^{138}Ce for which final J^{π} values are known. The proton[15] (P1) and triton[33] (T1) optical model parameters of Table IV were used. Form factors were constructed for 0^+ and 2^+ levels utilizing the $(1h_{11/2})^2$ and $(2d_{3/2})^2$ single particle wave functions according to Ref. 27. The bound state geometry is included in Table IV.

The results for the two form factors are shown for the ^{140}Ce ground (0^+) and 1.595 MeV (2^+) levels in Fig. 4. The solid curve used the $(1h_{11/2})^2$ form factor, and the dashed curve corresponds to the $(2d_{3/2})^2$ form factor. Similar calculations are shown for the ^{140}Ce(p,t) reaction leading to the ^{138}Ce ground (0^+) and 0.788 MeV (2^+) levels in Fig. 6. Both form factors give good agreement for the angular distribution shape in each case. Discussion of the DWBA normalizations for each of these two form factors is given in the next section.

The effect of varying Q-values has sizable influence on the shape of the DWBA predictions. Figure 7 illustrates this Q-value effect for the L = 2, 3, and 4 transitions; a shift of the first maximum to larger angles as the Q-value becomes more negative is seen. Such a shift for the L = 4 case is experimentally observed in the (p,t) transitions to the ^{140}Ce(2.080 MeV) and ^{138}Ce (1.822 MeV) states, whose Q-values are -6.2 MeV and -10.0 MeV, respectively. However, detailed empirical comparisions of experimental angular distributions directed towards examining Q-effects are difficult, and the DWBA must be relied upon to describe this effect for the L = 3 and L = 4 transitions. Higher L transfers, such as the 7^- level at 2.130 MeV in ^{138}Ce, are not accurately described by DWBA calculations at forward angles. It is thus difficult to make restrictive assignments for levels whose angular distributions are characteristic of $L \gtrsim 6$. Fig. 7 also shows that, for a given Q-value, adjacent L values are similar at c.m. angles beyond about 16°.

2. Enhancement Factors

A method of obtaining spectroscopic information from absolute two-nucleon transfer cross sections by analyzing with zero-range DWBA is possible by using the empirical normalization (N) of Flynn and Hansen[34] with the enhancement factor[35] (ε) defined by

$$\sigma_{exp}(\Theta) = N\varepsilon\, \sigma_{DW}(\Theta). \qquad (3)$$

We used the value N = 218 obtained from Ref. 34; this is consistent with the (p,t) work on the titanium,[25] and zirconium[36] isotopes. However, several (t,p) works[34,37] have shown that the normalization N depends strongly on the choice of parameters used in the DWBA calculation, so our choice of N = 218 requires that our parameters be chosen in a manner consistent with the prescription given in Ref. 34.

Since the magnitude of $\sigma_{DW}(\Theta)$ is sensitive to the two neutron wave function,[26] one may expect ε to vary substantially with the choice of configuration. This is illustrated by comparing the values of ε extracted from the ground and first excited states in ^{138}Ce and ^{140}Ce assuming a $(1h_{11/2})^2$ or a $(2d_{3/2})^2$ configuration. For N = 218, the results are listed in Tables II and III with the $\varepsilon[(1h_{11/2})^2]$ given first, followed by the $\varepsilon[(2d_{3/2})^2]$ given in square brackets. For both ^{140}Ce and ^{138}Ce, the $\varepsilon[(1h_{11/2})^2]$ values are considerably larger than those found with the $(2d_{3/2})^2$ configuration.

3. Energy Dependence

The ^{142}Ce(p,t)^{140}Ce ground state (L=0) and 3.73 MeV (L=2) angular distributions have now been studied at 21.5 MeV[3], 30.3 MeV, and 52.1 MeV.[1] These data therefore offer an opportunity to check the adequacy of zero-range DWBA in describing the energy dependence of two-nucleon transfer reactions. Other investigations of this topic have been made previously.[25,38,39]

The L = 0 and L = 2 (p,t) angular distributions from the present work and those from Refs. 1 and 3 were analyzed by forming the ratio $R = \sigma_{exp}(\Theta)/\sigma_{DW}(\Theta)$. The calculations used the $(1h_{11/2})^2$ bound state form factor described previously. Three sets of triton optical model potentials, listed in Table IV, were tested in conjunction with proton set P1. The results of the calculations are given in Table V. A change of approximately 16:4:1 occurs for the $^{142}Ce(p,t)^{140}Ce(0.0)$ L = 0 transition as the beam energy is changed from 21.5 MeV to 52.1 MeV. The R values for the L=2 transition at 3.73 MeV over the same energy range change from 6:2.5:1. These ratios, with the exception of set P1-T2 for the 52.1 MeV data, are reasonably independent of the optical model parameters.

This energy dependence may be related to momentum mismatch in the (p,t) reaction[39] which may not be properly described by the zero-range DWBA. At 21.5, 30.3, and 52.1 MeV the proton and triton grazing partial waves (where $\eta_\ell = 0.5$) for the L = 2 transition differ by 2, 5, and 9, respectively. These values are one unit greater for the transition to the ^{140}Ce ground state. Thus, good angular momentum matching is not obtained in either case for this range of incident proton energies.

4. Spectroscopic Results from $^{142}Ce(p,t)^{140}Ce$

The triton differential cross sections from the $^{142}Ce(p,t)$ reaction have been systematically analyzed with the zero-range DWBA theory in order to derive L transfers, suggest J^π assignments, and extract enhancement factors. Form factors for positive and negative parity transitions were constructed assuming the $(1h_{11/2})^2$ and $(1h_{11/2}1g_{7/2})$ configurations, respectively, with the exception of the L = 1 transfers, for which the $(1h_{9/2}1g_{7/2})$ configuration was assumed. The $1h_{11/2}$ and $1g_{7/2}$ neutron hole states have been observed with large spectroscopic factors in the $^{140}Ce(p,d)$ reaction.[41]

While it is sometimes impossible to make unambiguous L assignments to experimental data based on DWBA angular distribution shapes, L=0 transitions are virtually always identifiable. Figure 7 shows that forward angle data (not obtained here) would be most valuable for L assignments. Wherever ambiguities arise, DWBA predictions for both of the possible L transfers are shown in Figs. 4 and 5 with the derived enhancement factors given in Table II. The DWBA calculations used the P1 and T1 optical model potentials and bound state parameters of Table IV and the zero-range normalization N = 218.

The ^{140}Ce results naturally separate into low excitation ($\lesssim$ 3.5 MeV) and high excitation ($\gtrsim$ 3.5 MeV) regions. In the former region considerable information exists from decay data[11,12,42], inelastic scattering[5], and proton transfer work.[43] Above 3.5 MeV excitation, most energy level information is derived from two-neutron transfer results and those from the ^{139}La(^{3}He,d) reaction.[43] While the ^{142}Ce(p,t) data at 21.5 MeV did not populate states above 4.8 MeV excitation, the current data yield level structure up to 6.4 MeV. The ^{142}Ce(p,t)^{140}Ce data are characterized by a strong L = 0 ground state transition with weak excitation of levels up to the 3.23 MeV 0^+ state. Above this excitation, strong transitions are observed in both (p,t) and (t,p) experiments.[1,3] In general our results (Table II) agree with previous information, with the exceptions noted below.

In the 2.0 to 2.5 MeV region several closely spaced levels exist which could not be resolved in this experiment. The 2.08 MeV level is most consistent with an L = 4 DWBA shape, indicating that the contribution from the 2.108 MeV state [$J^{\pi} = (6)^+$] is small. There is no evidence for the population of the unnatural-parity (3^+) state at 2.412 MeV, although it would have been resolved from the nearby 2.47 MeV level. A cross section of $\lesssim$ 0.5 μb/sr is an upper limit for exciting this state. The 2.471 MeV angular distribution was not well fit by any single L transfer, and is probably a doublet made up of the 2.464 and 2.481 MeV states. The 2.912 MeV level has an L=2 shape and thus we suggest that this

level be assigned $J^{\pi} = 2^{+}$. We associate this state with the 2.8997 MeV level assigned $(1,2)^{+}$ in the decay data.

The 3.026 MeV level has the characteristic L=0 angular distribution shape implying $J^{\pi} = 0^{+}$. This state is probably the same as the 3.04 MeV level which was excited in the (α,α') experiment.[5] The 3.334 MeV angular distribution is not characteristic of any natural-parity transition. This weak level [1-3μb/sr] might be associated with the 3.3197 $(1,2)^{+}$ level observed in the decay data, and is the most likely candidate in our data for the excitation of an unnatural-parity state.

Sixteen possible L=2 transitions are found in this work, ranging from 3.558 MeV to 6.187 MeV excitation, that were not reported earlier (see Figs. 4 and 5 and Table II). Quite possibly, at least some of these transitions have L=3. This ^{142}Ce(p,t) analysis has also revealed possible L=1 transfers to states at 4.242, 5.703, and 5.896 MeV in ^{140}Ce. These angular distributions are fit fairly well with L=1 DWBA calculations, implying $J^{\pi} = 1^{-}$ assignments, although L=2 assignments cannot be excluded. A $J^{\pi} = 1^{-}$ state might arise from the $(1h_{9/2}1g_{7/2})_{1^{-}}$ configuration, since the $(1h_{9/2})^{2}$ configuration is probably mixed weakly into the ^{142}Ce (g.s.) wave function.[44] No such L=1 shapes are observed in the ^{138}Ce spectrum (see below) nor are they expected, since the ^{140}Ce nucleus closes a major neutron shell below the $(1h_{9/2})$ orbital.

Above 3.23 MeV we find evidence for nine possible L=4 or L=5 transitions. We also tentatively assign L=0 to a state at 5.574 MeV. The rapid forward angle rise of the 5.574 MeV angular distribution is characteristic of an L = 0 transition, although at large angles the data do not agree very well with an L=0 shape. A coupled pair vibration model analysis[2] predicts L=0 strength in this region.

Higher L transfers ($L \geq 6$) are characterized by comparatively flat, featureless angular distributions. In Fig. 5 for example, the empirical L=7 shape taken from the $^{140}Ce(p,t)$ reaction is compared with the 5.101 MeV state, and L=5 and L=6 DWBA predictions are shown for the 5.295 MeV level. These angular distributions are much flatter (especially at forward angles) than those of the (L=3,4) 4.296 or 6.364 MeV levels.

Summarizing, we find that over the angular range studied here it is probably impossible, with the exception of L=0 transitions, to make unique L assignments based on shapes derived from DWBA calculations. However, limits of two possible L values can usually be made, and valuable conclusions regarding restricted J^{π} values can then be made for many states.

5. Spectroscopic Results from $^{140}Ce(p,t)^{138}Ce$

Table III summarizes states observed in the $^{140}Ce(p,t)$ reaction, as well as the DWBA analysis of their angular distributions. The DWBA prescriptions used are the same as those given in the previous section. The decay data,[13,45,46] included in Table III, give J^{π} information for the low-lying states. The $^{140}Ce(p,t)$ analysis is consistent with every assignment; the only exception is that the (p,t) data show no evidence for the 1.477 MeV 0^+ state.[13,46] This level would not have been resolved from the 1.501 MeV transition, and apparently is weakly excited in (p,t) since the 1.501 MeV state shows a pure L=2 transition (see Fig. 6). Possible L=2 or L=3 strength lies at 2.640, 2.885, 3.220, and 3.356 MeV (see Table III), although, as for the $^{142}Ce(p,t)^{140}Ce$ case, the DWBA calculations do not give conclusive L assignments. The 2.389 and 3.277 MeV levels were poorly resolved from neighboring excited states. While these angular distributions do not agree particularly well with any DWBA curve, comparisons to the most plausible L values are shown in Fig. 6. These are listed in Table III in parentheses, indicating uncertain assignments. Transitions characterized by L=4 or L=5 occur at 2.440,

2.719, 2.942, 3.005, 3.082, and 3.429 MeV. The fits to the 3.005 and 3.429 MeV levels, while not conclusive, are clearly better described by L=4 than L=5.

The decay data assign the 2.130 MeV state $J^{\pi} = 7^{-}$ and the 2.219 MeV state as J = 5, 6. The L=7 DWBA curve predicts very well the maximum in the 2.130 MeV angular distribution at 45° (although it fails at more forward angles), while the 2.219 MeV angular distribution is consistent with $L > 4$. Comparison with the empirical 2.130 MeV angular distribution shows that the 3.646 MeV level is also consistent with an L=7 assignment. The 3.531 MeV state is not characteristic of any natural-parity level and is probably due to a group of unresolved states. No likely candidates for L=1 strength were found in this study of ^{140}Ce(p,t).

C. Pairing Vibration Scheme

Analysis of the ^{142}Ce(p,t) and ^{140}Ce(p,t) reactions within the pairing vibration model[4] has been given in earlier work.[1-3] The lowest-order harmonic model predicts that a $J^{\pi} = 0^{+}$ state in ^{140}Ce should be excited in the (p,t) reaction with the same Q-value and strength as the ^{138}Ce (g.s.). The 0^{+} strength is known to be fragmented,[2,3] and this division of 0^{+} strength was previously discussed[2] for ^{140}Ce using a coupling model.[47] The monopole pairing model can be extended to include quadrupole pairing phonons, the latter being represented by the 0.788 MeV L=2 transiton from the ^{140}Ce(p,t) reaction. A more complete discussion of these ideas applied to the Ce nuclei is found in Refs. 1-3.

Table VI summarizes the L=0 and L=2 strength found in the present ^{142}Ce(p,t) work. The L=2 strength listed in Table VI corresponds to the L=2 assignments given in Ref. 3, with the addition of the 3.558 MeV level. The enhancement factors derived from the DWBA calculations using the $(1h_{11/2})^2$ form factor are also given here, along with their sum for the excited states given in the final column. The 3.233 MeV and 3.731 MeV states are candidates[1-3] for the expected pairing monopole and quadrupole excitations, but their

enhancement factors are considerably less than the ε values of 19.3 and 18.3 found for the ^{138}Ce (g.s.) and ^{138}Ce (0.788 MeV) transitions, respectively. However if the enhancement factors for the weaker 0^+ and 2^+ transitions are added, much better agreement is found. Two values of the summed L=0 enhancement factors (corresponding to retaining the 5.574 MeV (0^+) transition in the sum and deleting it) are given. Inclusion of the 5.574 MeV strength gives a very good agreement with the ^{138}Ce (g.s.) transition. Summing the L=2 fragments listed in Table VI gives similar improvement for the comparison with the ^{138}Ce (0.788 MeV) strength.

IV. SUMMARY

The ^{140}Ce(p,p') and ^{142}Ce(p,t) reactions have been used to study the ^{140}Ce nucleus. The (p,p') work gives results similar to the isoscalar excitation[5] of the ^{140}Ce even-parity collective levels, with differences noted for the odd-parity transitions. The ^{142}Ce(p,t) reaction has resulted in finding many new levels at excitations $\gtrsim$ 3.5 MeV in ^{140}Ce, as well as placing limits on their J^π values. The zero-range DWBA has been examined using the ^{142}Ce(p,t)^{140}Ce reaction at three incident proton energies, and we find it does not describe the variation of cross section with energy for L = 0 and L = 2 transitions. Three different optical model choices were used in this analysis.

The ^{140}Ce(p,t) reaction was also studied and yielded new information regarding the energy levels and possible J^π assignments for $E_x \geq 2.3$ MeV. The combined ^{142,140}Ce(p,t) results are consistent with pairing vibration model predictions for (p,t) transition strengths only if the weak L=0 and L=2 fragments observed in the ^{142}Ce(p,t) reactions are summed with the principle L=0 and L=2 excitations.

V. ACKNOWLEDGMENTS

We would like to thank C. Ellsworth for help in preparing the targets. One of us (JDS) acknowledges the support of Carnegie-Mellon University during the preparation of this paper. We also acknowledge a helpful discussion with N. S. P. King on the energy dependence of the (p,t) reaction.

FOOTNOTES AND REFERENCES

*Work performed under the auspices of the U.S. Energy Research and Development Administration.

†Present address, Carnegie-Mellon University Users Group, Clinton P. Anderson Meson Physics Facility, Los Alamos, N. M. 87545.

1. K. Yagi, Y. Aoki, and K. Sato, Nucl. Phys. A149, 45 (1970).
2. J. D. Sherman, B. G. Harvey, D. L. Hendrie, M. S. Zisman, and B. Sørensen, Phys. Rev. C 6, 1082 (1972).
3. T. J. Mulligan, E. R. Flynn, Ole Hansen, R. F. Casten, and R. K. Sheline, Phys. Rev. C 6, 1802 (1972).
4. A. Bohr, in Proceedings of the International Symposium on Nuclear Structure, Dubna, 1968 (International Atomic Energy Agency, Vienna, Austria, 1969).
5. F. T. Baker and R. Tickle, Phys. Rev. C 5, 182 (1972).
6. D. Larson, S. M. Austin, and B. H. Wildenthal, Phys. Letters 41B, 145 (1972).
7. D. Larson, S. M. Austin, and B. H. Wildenthal, Phys. Rev. C 9, 1574 (1974).
8. J. D. Sherman , Nucl. Instr. Methods, 135, 391 (1976).
9. R. E. Hintz, F. B. Selph, W. S. Flood, B. G. Harvey, F. G. Resmini, and E. A. McClatchie, Nucl. Instr. Methods 72, 61 (1969).
10. F. S. Goulding, D. A. Landis, J. Cerny, and R. H. Pehl, Nucl. Instr. Methods 31, 1 (1964).
11. H. W. Baer, J. J. Reidy, and M. L. Wiedenbeck, Nucl. Phys. 86, 332 (1966).
12. H. W. Baer, J. J. Reidy, and M. L. Wiedenbeck, Nucl. Phys. A113, 33 (1968).
13. G. M. Julian and T. E. Fessler, Phys. Rev. C 3, 751 (1971).
14. A. H. Wapstra and N. B. Gove, Nucl. Data Tables 9, 265 (1971).
15. F. D. Becchetti and G. W. Greenlees, Phys. Rev. 182, 1190 (1969).

16. R. H. Bassel, G. R. Satchler, R. M. Drisko, and E. Rost, Phys. Rev. 128, 2693 (1962).

17. P. D. Kunz, code DWUCK74. (unpublished)

18. Norman Austern, Direct Nuclear Reaction Theories, John Wiley and Sons (1970).

19. M. P. Fricke and G. R. Satchler, Phys. Rev. 139, 567 (1965).

20. E. R. Flynn and R. H. Bassel, Phys. Letters 15, 168 (1965).

21. H. W. Broek, J. L. Yntema, B. Buck, and G. R. Satchler, Nucl. Phys. 64, 259 (1965).

22. N. Austern and J. S. Blair, Annals of Phys. 33, 15 (1965).

23. A. M. Bernstein, Adv. in Nucl. Phys. 3, 325 (1969).

24. R. Pitthan, Z. Naturforsch, 25a, 1358 (1970).

25. H. W. Baer, J. J. Kraushaar, C. E. Moss, N. S. P. King, R. E. L. Green, P. D. Kunz, and E. Rost, Annals of Phys. 76, 437 (1973).

26. N. K. Glendenning, Phys. Rev. 137, 102 (1965).

27. B. F. Bayman and A. Kallio, Phys. Rev. 156, 1121 (1967).

28. I. S. Towner and J. C. Hardy, Advances in Phys. 18, 401 (1969).

29. R. J. Ascuitto and N. K. Glendenning, Phys. Rev. C 2, 1260 (1970).

30. R. J. Ascuitto, N. K. Glendenning, and B. Sørensen, Phys. Letters 34, 17 (1971).

31. B. F. Bayman and D. H. Feng, Nucl. Phys. A205, 513 (1973).

32. N. S. Chant, Nucl. Phys. A211, 269 (1973).

33. E. R. Flynn, D. D. Armstrong, J. G. Beery, and A. G. Blair, Phys. Rev. 182, 1113 (1969).

34. E. R. Flynn and O. Hansen, Phys. Letters 31B, 135 (1970).

35. R. A. Broglia, O. Hansen, C. Riedel, Adv. in Nucl. Phys. 6, 287 (1974).

36. J. Ball, R. Auble, and P. Roos, Phys. Rev. C 4, 196 (1971).

37. E. R. Flynn, J. D. Sherman, N. Stein, D. K. Olsen, and P. J. Riley, Phys. Rev. C 13, 568 (1976); E. R. Flynn, O. Hansen, J. D. Sherman, N. Stein, and J. W. Sunier, Nucl. Phys. A264, 253 (1976).

38. S. W. Cosper, H. Brunnader, J. Cerny, and R. L. McGrath, Phys. Lett. 25B, 324 (1967).

39. M. Pignanelli, S. Micheletti, I. Iori, P. Guazzoni, F. G. Resmini, and J. L. Escudie, Phys. Rev. C 10, 445 (1974).

40. F. D. Becchetti, Jr. and G. W. Greenlees, in Polarization Phenomena in Nuclear Reactions, ed. by H. H. Barschall and W. Haeberli, University of Wisconsin Press, Madison, 1971, p. 682.

41. K. Yagi, T. Ishimatsu, Y. Ishizaki, and Y. Saji, Nucl. Phys. A121, 161 (1968).

42. S. E. Karlsson, B. Svahn, H. Pettersson, G. Malmsten, and E. Y. De Aisenberg, Nucl. Phys. A100, 113 (1967).

43. W. P. Jones, L. W. Borgman, K. T. Hecht, John Bardwick, and W. C. Parkinson, Phys. Rev. C 4, 580 (1971).

44. R.H. Fulmer, A. L. McCarthy, and B. L. Cohen, Phys. Rev. 128, 1302 (1962).

45. M. Fujioka, K. Hisatake, and K. Takahashi, Nucl. Phys. 60, 294 (1964); H. Nakayama, M. Fujioka, K. Hisatake, Journal of Phys. Soc. (Japan) 24, 623 (1968).

46. K. Gromow, et al. Nucl. Phys. 88, 225 (1966).

47. B. Sørensen, Nucl. Phys. A177, 465 (1971).

Table I. Comparison of ^{140}Ce collective levels seen in (p,p') and (α,α').

$^{140}Ce(p,p')$				$^{140}Ce(\alpha,\alpha')^a$			
E_x^b (MeV)	J^π	δ_L^c (fm)	G_{IS}^d (spu)	E_x (MeV)	J^π	δ_L (fm)	G_{IS}^d (spu)
1.589	2^+	0.41	5.8	1.597	2^+	0.46	7.4
2.094	4^+	0.43	6.9	2.09	4^+	0.42	6.8
				2.35	(2^+)	0.08	0.22
2.469	3^-	0.79	22.1	2.464	3^-	0.67	15.8
2.902	2^+	0.15	0.76	2.90	2^+	0.13	0.55
				3.04	3^-	0.15	0.80
3.130	2^+	0.26	2.3	3.12	2^+	0.22	1.7
3.264	5^-	0.12	0.58	3.25	5^-	0.30	3.6
				3.34	4^+	0.24	2.2
				3.54	$(4)^+$	0.21	1.7
				3.98	3^-	0.21	1.56

[a] Ref. 5.

[b] All excitation energies ± 0.01 MeV

[c] $\delta_L = \beta_L R_R$, $R_R = 1.17\ A^{1/3}$

[d] Isoscalar transition rate in single particle units assuming a sharp edge mass distribution.

Table II. Summary of the ^{142}Ce(p,t) results.

Level No.	^{142}Ce(p,t) E_p = 30 MeV This Work E_x[b] (MeV)	L	Suggested J^π	ε[c]	^{142}Ce(p,t) E_p = 21.5 MeV Ref. 3 E_x (MeV)	L	Decay data[a] E_x (MeV)	J^π
1	0.0	0	0^+	19.3 [3.4]	0.0	0	0.0	0^+
2	1.595	2	2^+	2.3 [0.50]	1.600	2	1.5966	2^+
3	1.905	0	0^+	2.1	1.906	0	1.9035	0^+
4	2.080	4	4^+	0.28			2.0836	4^+
	2.107						2.1082	$(6)^+$
							2.3484	2^+
							2.3502	$(5)^-$
							2.4124	3^+
5	2.471				2.468		2.4644	3^-
							2.4813	$(4)^+$
6	2.519	3,4	$3^-,4^+$	2.1,0.22			2.5161	$(4^+,3^+,3^-)$
							2.5218	2^+
							2.5475	$(1,2)^+$
7	2.912	2	2^+	0.46			2.8997	$(1,2)^+$
8	3.026	0	0^+	1.1	3.020			

(continued)

Table II. (Continued)

Level No.	^{142}Ce(p,t) E_p = 30 MeV This Work E_x[b] (MeV)	L	Suggested J^π	ε[c]	^{142}Ce(p,t) E_p = 21.5 MeV Ref. 3 E_x (MeV)	L	Decay data[a] E_x (MeV)	J^π
							3.1183	$(1,2)^+$
9	3.134	2,3,4						
10	3.233	0	0^+	13.8	3.223	0		
11	3.334						3.3197	$(1,2)^+$
12	3.426							
13	3.558	2,3	$2^+,3^-$	1.7,10.3	3.540			
14	3.664	2,3	$2^+,3^-$	1.3,8.7	3.654	2		
					3.709			
15	3.731	2,3	$2^+,3^-$	13.3,68.8	3.731	2		
					3.744			
16	3.801	2,3	$2^+,3^-$	1.6,10.6				
17	3.911	4,5	$4^+,5^-$	0.41,0.82				
18	3.985	2,3	$2^+,3^-$	1.7, 10.1	3.965	2		
19	4.017							
20	4.125	2,3	$2^+,3^-$	1.1,7.8	4.123	2		
21	4.183	2,(3,4)	$2^+,(3^-,4^+)$	1.3	4.188	2		

(continued)

Table II. (continued)

Level No.	^{142}Ce(p,t) E_p = 30 MeV This Work E_x[b] (MeV)	L	Suggested J^π	ε[c]	^{142}Ce(p,t) E_p = 21.5 MeV Ref. 3 E_x (MeV)	L	Decay data[a] E_x (MeV)	J^π
22	4.242	1,2	$1^-,2^+$	4.6,1.8	4.242			
23	4.296	3,4	$3^-,4^+$	12.4,1.2	4.301			
24	4.360							
25	4.431	2,3	$2^+,3^-$	1.1,7.8	4.429			
26	4.534	2,3	$2^+,3^-$	1.2,8.7				
27	4.758							
28	4.827	2,3	$2^+,3^-$	10.6,68.8	4.831	2		
29	4.979	2,3	$2^+,3^-$	4.6,29.4				
30	5.101	$L \geqslant 5$						
31	5.157							
32	5.229	2,3,4	$2^+,3^-,4^+$					
33	5.295	5,6	$5^-,6^+$	5.0,2.1				
34	5.377	4,5	$4^+,5^-$	2.3,5.5				
35	5.449							
36	5.574±15 keV	(0)	(0^+)	(2.3)				
37	5.650	2,3	$2^+,3^-$	1.7,11.0				

(continued)

Table II. (continued)

Level No.	E_x[b] (MeV)	^{142}Ce(p,t) E_p = 30 MeV This Work L	Suggested J^π	ε[c]	^{142}Ce(p,t) E_p= 21.5 MeV Ref. 3 E_x (MeV)	L	Decay data[a] E_x (MeV)	J^π
38	5.703	1,2	$1^-,2^+$	6.0,2.1				
39	5.789	2,3,4						
40	5.896	1,2	$1^-,2^+$	6.9,2.3				
41	5.989	(3,4)	$(3^-,4^+)$	(15.1,1.5)				
42	6.078	2,3	$2^+,3^-$	3.0,21.1				
43	6.187	2,3	$2^+,3^-$	2.1,13.8				
44	6.268	3,4,5						
45	6.364	3,4	$3^-,4^+$	18.3,2.1				

[a] Ref. 11, 12, 42.

[b] Relative excitation energies ± 10 keV below level 36, ± 15 keV above level 36.

[c] Values in square brackets were obtained using the $(2d_{3/2})^2$ form factor, all others assumed a $(1h_{11/2})^2$ configuration. See text.

Table III. Summary of the ^{140}Ce(p,t) results.

Level No.	^{140}Ce(p,t)^{138}Ce E_p = 30 MeV This Work E_x^b (MeV)	L	Suggested J^π	ε^c	Decay data[a] E_x (MeV)	J^π
1	0.0	0	0^+	19.3 [3.7]	0.0	0^+
2	0.788	2	2^+	18.3 [4.6]	0.7888	2^+
					1.4770	0^+
3	1.501	2	2^+	3.0	1.5109	(2^+)
4	1.822	4	4^+	5.7	1.8264	4^+
5	2.130	7	7^-	4.6	2.1291	7^-
6	2.219	5,6	$5^-,6^+$	20.6,6.4	2.2173	5,6
					2.2368	
7	2.336	0	0^+	2.7	2.3403	
8	2.389	(2,3)	$(2^+,3^-)$	(1.3,8.7)		
9	2.440	4,5	$4^+,5^-$	1.3,3.7		
10	2.640	2,3	$2^+,3^-$	3.9,32.1		
11	2.719	4,5	$4^+,5^-$	0.92,2.6		
					2.765	
12	2.885	2,3	$2^+,3^-$	3.9,27.5		
13	2.942	4,5	$4^+,5^-$	4.1,11.5		
14	3.005	4,5	$4^+,5^-$	3.1,9.2		
15	3.082	4,5	$4^+,5^-$	0.78,2.1		
16	3.220	2,3	$2^+,3^-$	3.4,28.9		
17	3.277	(3)	(3^-)	21.6		
18	3.356	2,3	$2^+,3^-$	3.7,27.5		
19	3.429	4,5	$4^+,5^-$	1.2,3.9		
20	3.531					
21	3.646	(7)	(7^-)	1.8		

[a] Refs. 13, 45, 46

[b] Relative excitation energies ± 10 keV below level 7, ± 16 keV above level 7.

[c] Values in square brackets were obtained using the $(2d_{3/2})^2$ form factor, all others assumed a $(1h_{11/2})^2$ configuration. See text.

Table IV. Optical model potentials and bound state parameters used in the DWBA calculations. The form of the potentials and notation is that of Ref. 15.

	V_R^a (MeV)	r_R (fm)	a_R (fm)	W_V^a (MeV)	W_{SF}^a (MeV)	r_I (fm)	a_I (fm)	V_{SO} (MeV)	r_{SO} (fm)	a_{SO} (fm)	r_C (fm)	Spin Orbit Unit
P1[c]	$\left\{\begin{matrix}54.0-0.32E_p \\ +0.4Z/A^{1/3} \\ +24.0(N-Z)/A\end{matrix}\right\}$	1.17	0.75	$0.22E_p-2.7$	$\left\{\begin{matrix}11.8-0.25E_p \\ +12.0(N-Z)/A\end{matrix}\right\}$	1.32	0.63	6.2	1.01	0.75	1.21	
T1[d]	166.7	1.16	0.752	16.4	- -	1.498	0.817				1.21	
T2[e]	$138.8-0.157E_t$	1.10	0.853	- -	$\left\{\begin{matrix}37.4-0.52E_t \\ +0.0037(E_t)^2\end{matrix}\right\}$	1.308	0.751				1.25	
T3[f]	$\left\{\begin{matrix}165.0-0.17E_t \\ -6.4(N-Z)/A\end{matrix}\right\}$	1.20	0.72	$\left\{\begin{matrix}46.0-0.33E_t \\ -110(N-Z)/A\end{matrix}\right\}$		1.40	0.84				1.30	
Bound State	b	1.27	0.67									32.0

[a] The energy dependent potentials are evaluated at the appropriate laboratory energy.

[b] The single particle bound state potential depth is determined by binding each neutron at half the two-neutron separation energy.

[c] Ref. 15

[d] Ref. 33

[e] Ref. 25

[f] Ref. 40

Table V. Energy Dependendence of DWBA Calculations

Optical Potential Set[a]	$R^{b}_{21.5}$	$R^{b}_{30.3}$	$R^{b}_{52.1}$
	^{140}Ce(0.0 MeV); L = 0		
P1-T1	13	4.1	0.96
P1-T2	19	2.6	0.22
P1-T3	16	4.5	0.70
	^{140}Ce(3.73 MeV); L = 2		
P1-T1	5.5	2.8	1.2
P1-T2	9.0	2.4	0.3
P1-T3	6.8	2.8	1.0

[a] See Table IV.

[b] $R_{E_p} = \sigma_{exp}/\sigma_{DW}$. All entries have been multiplied by 10^{-3}. See text.

Table VI. Distribution of L = 0 and L = 2 strength in ^{140}Ce found in the ^{142}Ce(p,t) reaction.

E_x (MeV)	L	$\sigma(\Theta)$[a] (μb/sr)	ε	Σ[b]
0.0	0	135.	19.3	
1.905	0	13.5	2.1	
3.026	0	7.2	1.1	
3.233	0	105.	13.8	17.0
5.574	(0)	13.	(2.3)	(19.3)
3.558	2	32.	1.7	
3.664	2	32.	1.3	
3.731	2	290.	13.3	
3.985	2	35.	1.7	
4.125	2	23.	1.1	
4.183	2	21.	1.3	20.4

[a] The L = 0 cross sections are measured at $\Theta_\ell = 35°$, the L = 2 values are at $\Theta_\ell = 16°$.

[b] Sum of excited-state enhancement factors.

FIGURE CAPTIONS

Fig. 1. Representative $^{142}Ce(p,t)^{140}Ce$ triton spectrum. The ^{17}F peaks were used as calibration points.

Fig. 2. Representative $^{140}Ce(p,t)^{138}Ce$ triton spectrum.

Fig. 3. Angular distributions from the $^{140}Ce(p,p')$ reaction. The solid curves are DWBA calculations, while the dashed curves are empirical (p,p') angular distribution shapes taken from the literature.

Fig. 4. Angular distributions from the $^{142}Ce(p,t)^{140}Ce$ experiment for levels below 4.183 MeV. The solid and dashed curves are DWBA predictions, unless otherwise noted. Except for the L = 0 transitions, the angular distributions could usually be reasonably fit by more than one L transfer. See text for discussion.

Fig. 5. Angular distributions from the $^{142}Ce(p,t)^{140}Ce$ experiment for levels above 4.242 MeV. See caption to Fig. 4.

Fig. 6. Angular distributions extracted from the $^{140}Ce(p,t)^{138}Ce$ experiment. See caption to Fig. 4.

Fig. 7. DWBA calculations for the $^{142}Ce(p,t)^{140}Ce$ reaction as a function of Q-value for L=2,3, and 4 transitions. This figure exphasizes the usefulness of forward angle data ($\theta < 16^{\circ}$) in assigning L values by comparing experimental results with DWBA predictions.

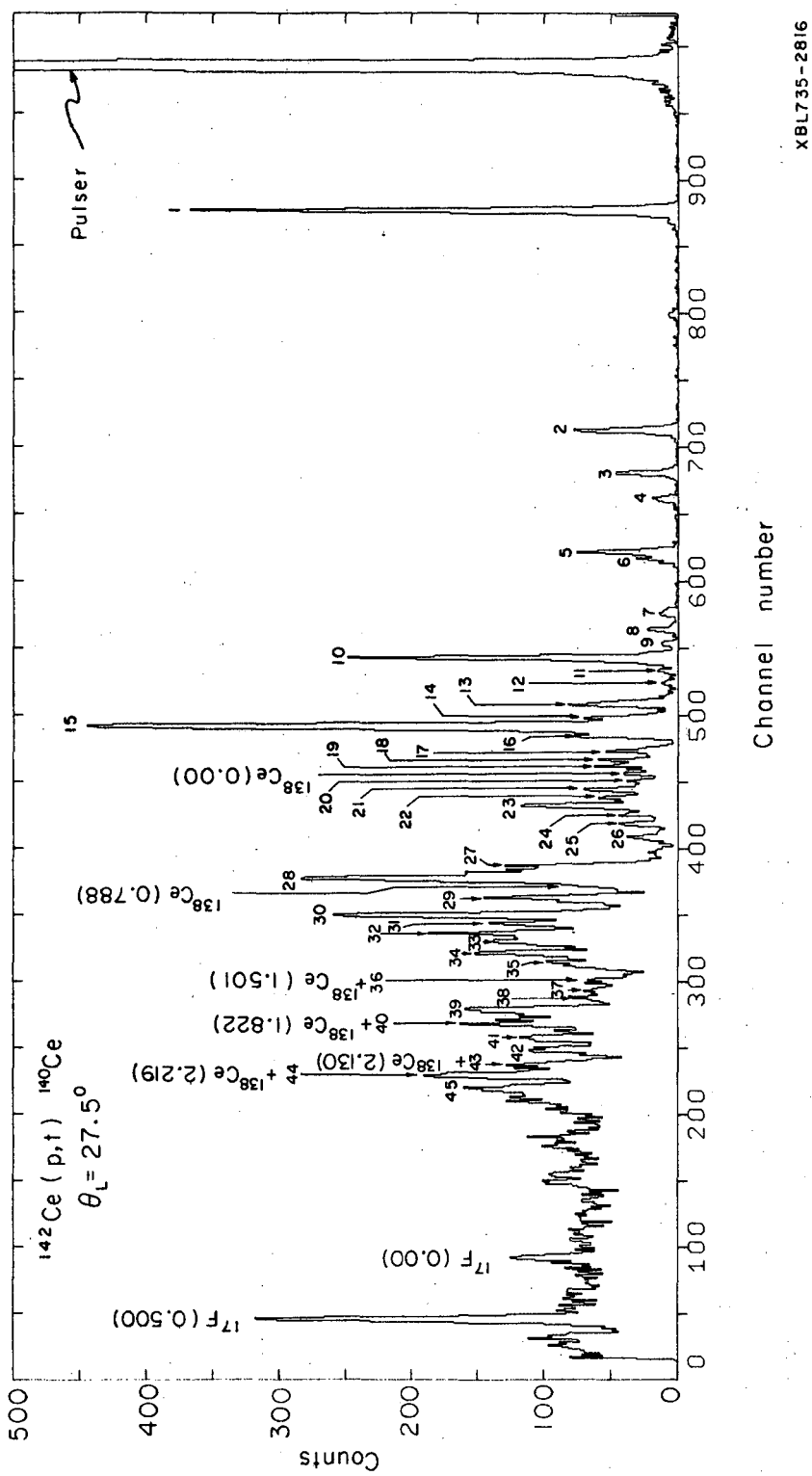
Counts
Channel number
^{142}Ce (p,t) ^{140}Ce
$\theta_L = 27.5^0$
Pulser
^{17}F (0.500)
^{17}F (0.00)
^{138}Ce (2.219)
^{138}Ce (2.130)
0^+ ^{138}Ce (1.822)
2^+ ^{138}Ce (1.501)
^{138}Ce (0.788)
^{138}Ce (0.00)
XBL735-2816

Fig. 1

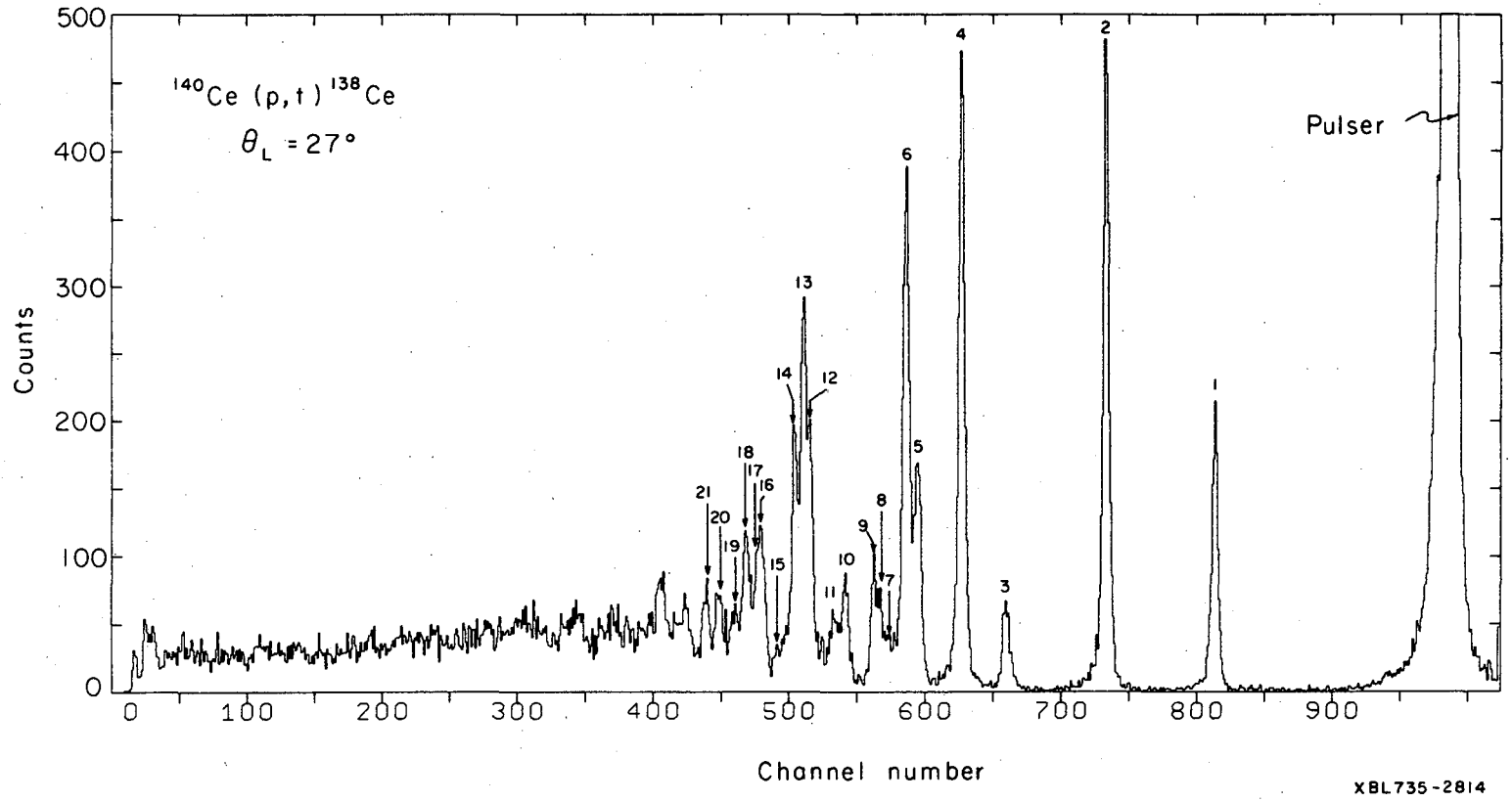
^{140}Ce (p,t) ^{138}Ce
θ_L = 27°
Pulser
Counts
Channel number
XBL735-2814
0
100
200
300
400
500
600
700
800
900
1
2
3
4
5
6
7
8
9
10
11
12
13
14
15
16
17
18
19
20
21

Fig. 2

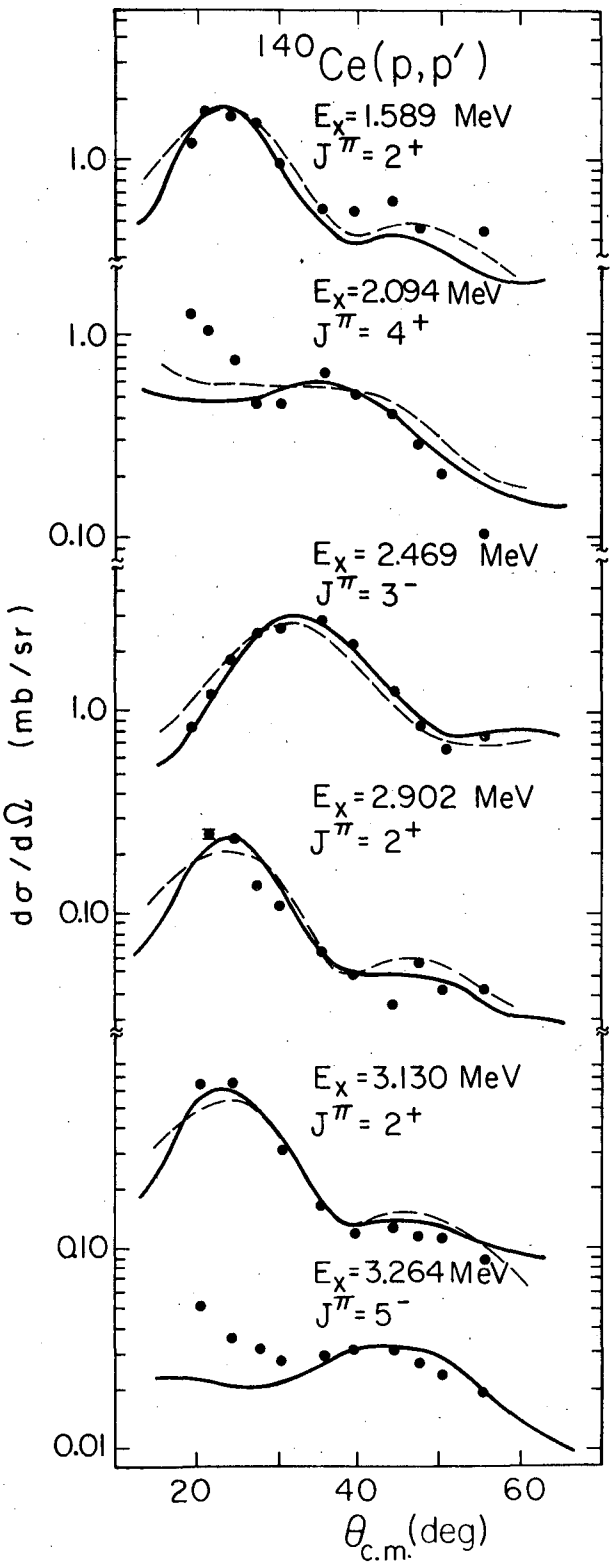

XBL 769-3938

Fig. 3

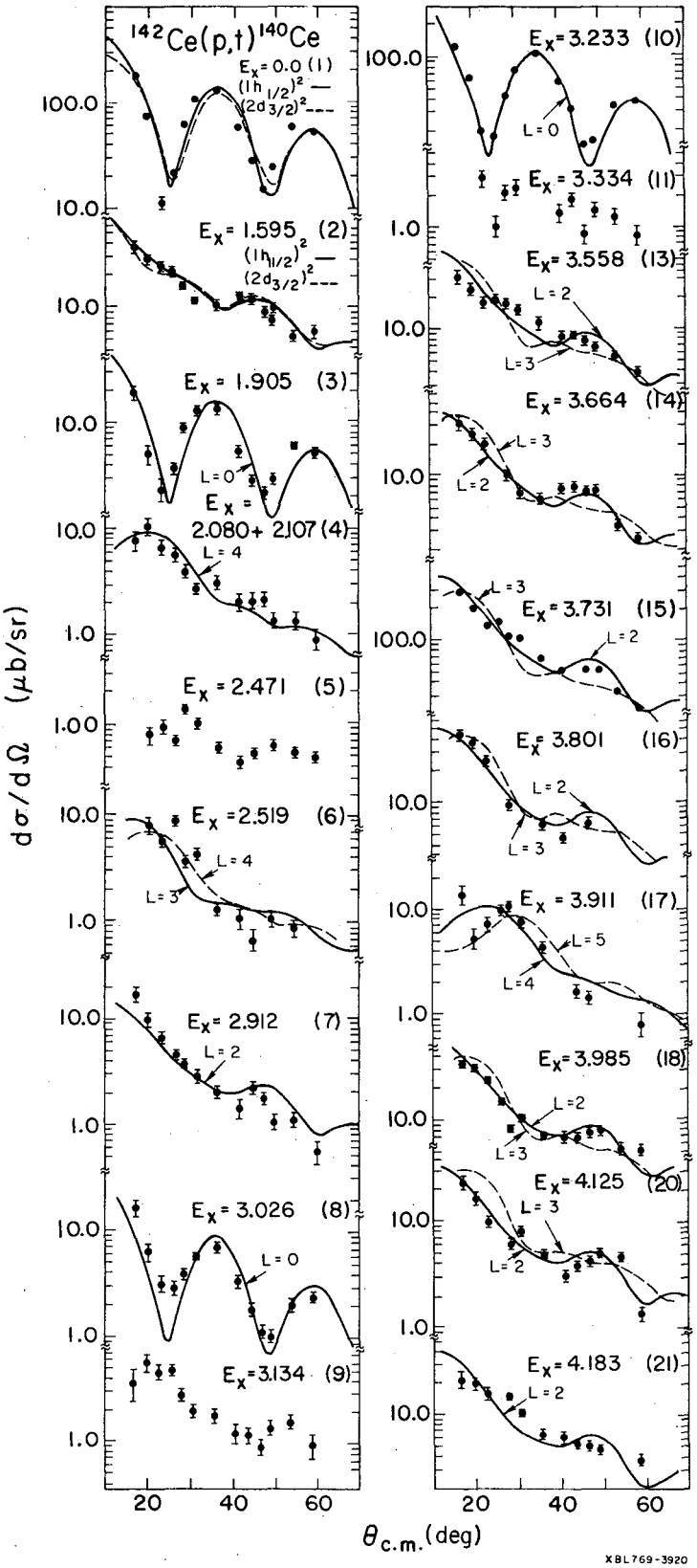
142Ce(p,t)140Ce
Ex = 0.0 (1)
(1h11/2)2 —
(2d3/2)2 ---
Ex = 1.595 (2)
(1h11/2)2 —
(2d3/2)2 ---
Ex = 1.905 (3)
L = 0
Ex = 2.080+ 2.107 (4)
L = 4
Ex = 2.471 (5)
Ex = 2.519 (6)
L = 4
L = 3
Ex = 2.912 (7)
L = 2
Ex = 3.026 (8)
L = 0
Ex = 3.134 (9)
Ex = 3.233 (10)
L = 0
Ex = 3.334 (11)
Ex = 3.558 (13)
L = 2
L = 3
Ex = 3.664 (14)
L = 3
L = 2
L = 3
Ex = 3.731 (15)
L = 2
Ex = 3.801 (16)
L = 2
L = 3
Ex = 3.911 (17)
L = 5
L = 4
Ex = 3.985 (18)
L = 2
L = 3
Ex = 4.125 (20)
L = 3
L = 2
Ex = 4.183 (21)
L = 2
dσ/dΩ (μb/sr)
θc.m.(deg)
XBL769-3920

Fig. 4

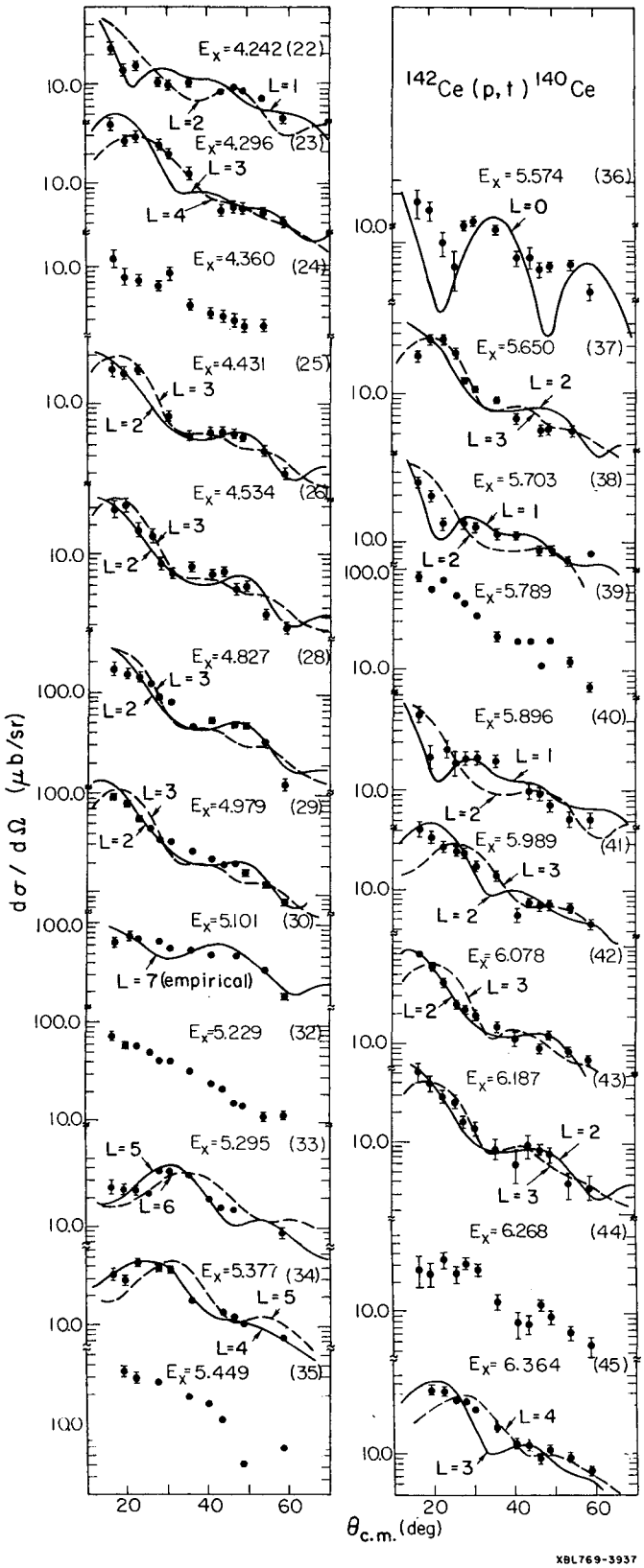
142Ce (p, t) 140Ce
Ex=4.242 (22)
L=1
L=2
Ex=4.296 (23)
L=3
L=4
Ex=4.360 (24)
Ex=4.431 (25)
L=3
L=2
Ex=4.534 (26)
L=3
L=2
Ex=4.827 (28)
L=3
L=2
Ex=4.979 (29)
L=3
L=2
Ex=5.101 (30)
L=7 (empirical)
Ex=5.229 (32)
Ex=5.295 (33)
L=5
L=6
Ex=5.377 (34)
L=5
L=4
Ex=5.449 (35)
Ex=5.574 (36)
L=0
Ex=5.650 (37)
L=2
L=3
Ex=5.703 (38)
L=1
L=2
Ex=5.789 (39)
Ex=5.896 (40)
L=1
L=2
Ex=5.989 (41)
L=3
L=2
Ex=6.078 (42)
L=3
L=2
Ex=6.187 (43)
L=2
L=3
Ex=6.268 (44)
Ex=6.364 (45)
L=4
L=3
dσ / dΩ (μb/sr)
θc.m. (deg)
XBL769-3937

Fig. 5

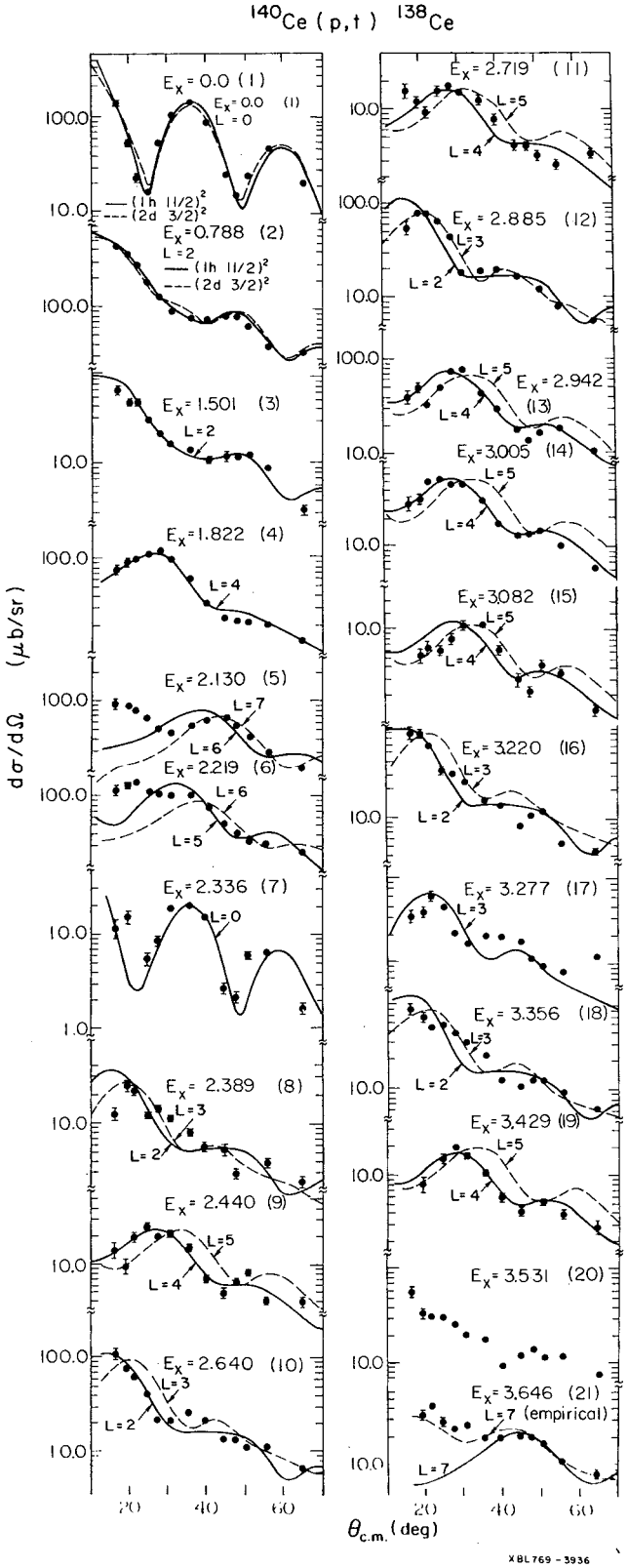
140Ce (p,t) 138Ce
Ex = 0.0 (1)
Ex = 0.788 (2)
Ex = 1.501 (3)
Ex = 1.822 (4)
Ex = 2.130 (5)
Ex = 2.219 (6)
Ex = 2.336 (7)
Ex = 2.389 (8)
Ex = 2.440 (9)
Ex = 2.640 (10)
Ex = 2.719 (11)
Ex = 2.885 (12)
Ex = 2.942 (13)
Ex = 3.005 (14)
Ex = 3.082 (15)
Ex = 3.220 (16)
Ex = 3.277 (17)
Ex = 3.356 (18)
Ex = 3.429 (19)
Ex = 3.531 (20)
Ex = 3.646 (21)
L = 0
L = 2
L = 3
L = 4
L = 5
L = 6
L = 7
L = 7 (empirical)
(1h 11/2)²
(2d 3/2)²
dσ/dΩ (μb/sr)
θc.m. (deg)
XBL769-3936

Fig. 6

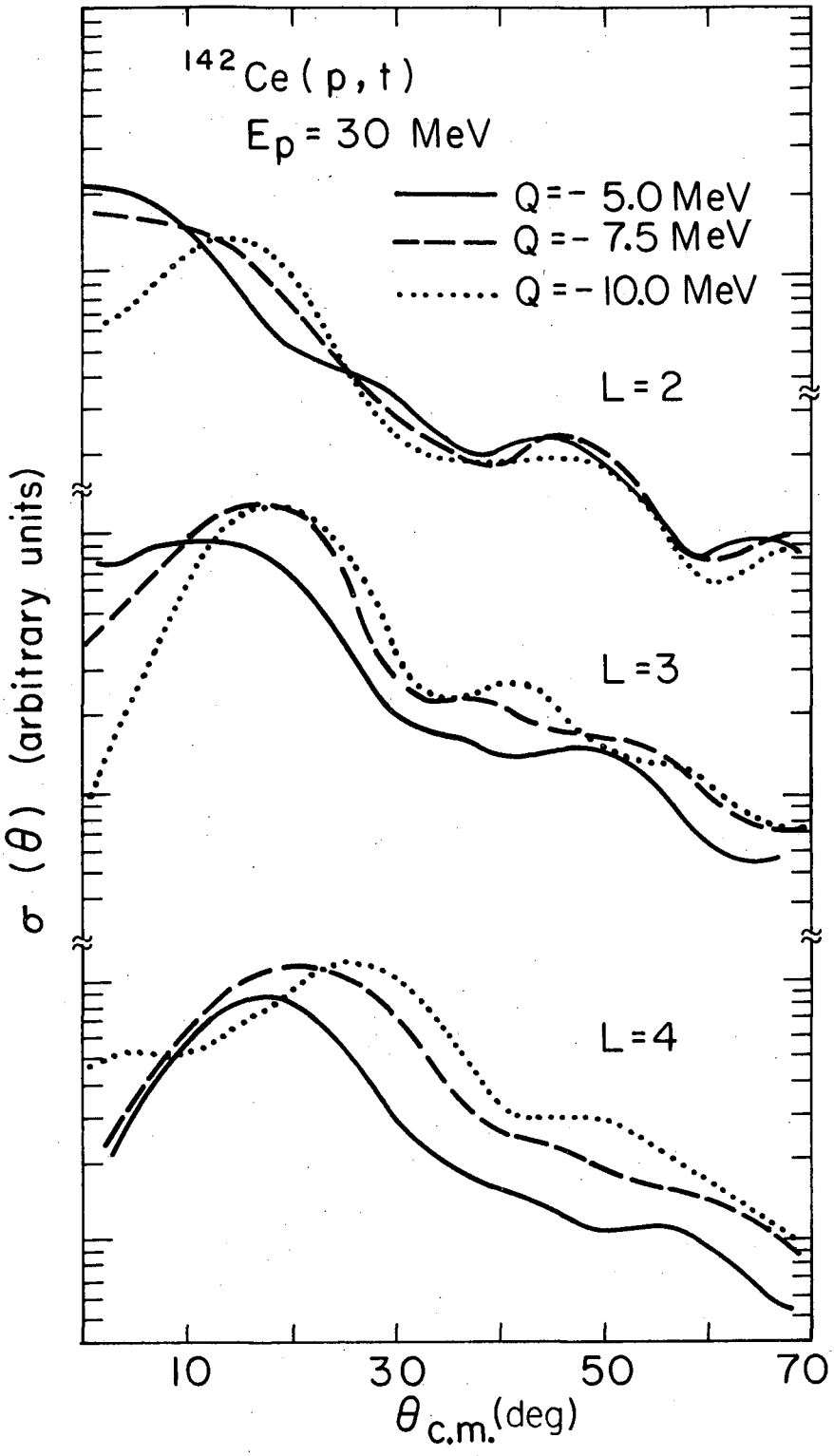

XBL768-3371

Fig. 7

This report was done with support from the United States Energy Research and Development Administration. Any conclusions or opinions expressed in this report represent solely those of the author(s) and not necessarily those of The Regents of the University of California, the Lawrence Berkeley Laboratory or the United States Energy Research and Development Administration.

TECHNICAL INFORMATION DIVISION
LAWRENCE BERKELEY LABORATORY
UNIVERSITY OF CALIFORNIA
BERKELEY, CALIFORNIA 94720